



UNIVERSITY OF LEEDS

This is a repository copy of *Preparation of Iron- and Nitrogen-Codoped Carbon Nanotubes from Waste Plastics Pyrolysis for the Oxygen Reduction Reaction*.

White Rose Research Online URL for this paper:  
<http://eprints.whiterose.ac.uk/155394/>

Version: Supplemental Material

---

**Article:**

Cai, N, Xia, S, Zhang, X et al. (7 more authors) (2020) Preparation of Iron- and Nitrogen-Codoped Carbon Nanotubes from Waste Plastics Pyrolysis for the Oxygen Reduction Reaction. *ChemSusChem*, 13 (5). pp. 938-944. ISSN 1864-5631

<https://doi.org/10.1002/cssc.201903293>

---

© 2019 Wiley-VCH Verlag GmbH & Co. KGaA, Weinheim. This is the peer reviewed version of the following article: N. Cai, S. Xia, X. Zhang, Z. Meng, P. Bartocci, F. Fantozzi, Y. Chen, H. Chen, P. T. Williams, H. Yang, *ChemSusChem* 2020, 13, 938, which has been published in final form at <https://doi.org/10.1002/cssc.201903293>. This article may be used for non-commercial purposes in accordance with Wiley Terms and Conditions for Use of Self-Archived Versions.

**Reuse**

Items deposited in White Rose Research Online are protected by copyright, with all rights reserved unless indicated otherwise. They may be downloaded and/or printed for private study, or other acts as permitted by national copyright laws. The publisher or other rights holders may allow further reproduction and re-use of the full text version. This is indicated by the licence information on the White Rose Research Online record for the item.

**Takedown**

If you consider content in White Rose Research Online to be in breach of UK law, please notify us by emailing [eprints@whiterose.ac.uk](mailto:eprints@whiterose.ac.uk) including the URL of the record and the reason for the withdrawal request.



[eprints@whiterose.ac.uk](mailto:eprints@whiterose.ac.uk)  
<https://eprints.whiterose.ac.uk/>

## **A new method for the preparation of iron and nitrogen co-doped carbon nanotubes from waste plastics pyrolysis for oxygen reduction reaction**

Ning Cai,<sup>[b]</sup> Sunwen Xia,<sup>[b]</sup> Xiong Zhang,<sup>[b]</sup> Zihan Meng,<sup>[c]</sup> Pietro Bartocci,<sup>\*,[a]</sup> Francesco Fantozzi,<sup>[a]</sup> Yingquan Chen,<sup>[b]</sup> Hanping Chen,<sup>[b]</sup> Paul T. Williams,<sup>[d]</sup> Haiping Yang,<sup>\*,[b]</sup>

**Abstract:** A novel method to prepare iron and nitrogen co-doped carbon nanotubes (Fe-N-CNT) is proposed, based on catalytic pyrolysis of waste plastics. At first carbon nanotubes are produced from pyrolysis of plastic waste over Fe-Al<sub>2</sub>O<sub>3</sub>; then Fe-CNT and melamine are heated together in inert atmosphere. Different co-pyrolysis temperatures are tested to optimize the electrocatalyst production. Working at a high doping temperature improved the degree of graphite formation and promoted the conversion of nitrogen to a more stable form. Compared with commercial platinum on carbon, the electrocatalyst obtained from pyrolysis at 850°C, showed remarkable properties, with onset potential of 0.943 V vs RHE and half-wave potential of 0.811 V vs RHE and even better stability and anti-poisoning. In addition, zinc-air batteries tests were also carried out and the optimized catalyst exhibited high maximum power density.

## Table of Contents

Section 1. Materials and Methods: page 1-3

Section 2. Results and discussion

Section 3. References

## Materials and Methods

The plastic waste used in this work consisted of used disposable lunch boxes made of polypropylene. They were crushed and mixed using a liquid nitrogen grinder with particle size between 0.1 and 0.5 cm. Proximate analysis and ultimate analysis of polypropylene are presented in the Table S1, and the main component was volatile matter.

Catalytic materials: iron nitrate ninehydrate ( $\text{Fe}(\text{NO}_3)_3 \cdot 9\text{H}_2\text{O}$ ), aluminum oxide ( $\gamma\text{-Al}_2\text{O}_3$ ), nanometer sized (10nm), and melamine ( $\text{C}_3\text{N}_3(\text{NH}_2)_3$ ) were purchased from Sigma Aldrich (China). Methanol and absolute ethyl alcohol were purchased from Sinopharm Chemical Reagent Co. Ltd. (China). 5% Nafion solution and 20% Pt/C were purchased from HESEN (Shanghai, China). All chemicals were of analytical grade and used without further purification. All aqueous solutions used in the experiments were prepared with ultra-pure water ( $>18 \text{ M}\Omega \text{ cm}^{-1}$ ) from a Millipore system and all electrochemical measurements were carried out at ambient temperature (25 °C).

Fe based catalyst was prepared with an impregnation method and  $\gamma\text{-Al}_2\text{O}_3$  was used as the support. Firstly, 7.21g  $\text{Fe}(\text{NO}_3)_3 \cdot 9\text{H}_2\text{O}$  was dissolved into 20 mL absolute ethyl alcohol, and 10.00 g of  $\gamma\text{-Al}_2\text{O}_3$  was added to ensure that the initial Fe loading was 10 wt.%. Then, the mixed solution was stirred for 4 h at 50 °C with a magnetic stirrer, then dried in an oven at 105 °C overnight, and followed by calcination at 800 °C for 2 h under air atmosphere with a heating rate of 10 °C  $\text{min}^{-1}$ . The catalyst was crushed and sieved to size smaller than 0.1 mm, which was labeled as Fe- $\text{Al}_2\text{O}_3$ .

Waste plastics catalytic pyrolysis was used to produce carbon nanotubes and the experiments were carried out in a two-stage fixed bed reactor. The experimental system mainly includes: a quartz reactor with two different heating zones (upper stage for pyrolysis, lower stage for catalysis and the temperatures were controlled separately), an inert gas supply system and an end gas treatment system. For the synthesis of Fe-CNT, 0.5 g Fe- $\text{Al}_2\text{O}_3$  was put into a quartz holder on the lower stage and 1 g plastic was put into another quartz holder on the upper stage. The lower stage was firstly preheated to the catalytic temperature of 800 °C with a heating rate of 20 °C  $\text{min}^{-1}$ . When the lower stage reached the set-point temperature, the plastic was introduced into the middle of the upper stage. Then, the upper stage was heated to 500 °C at 10 °C  $\text{min}^{-1}$  and was kept isothermal for 10 min. Meanwhile, at the end of the reactor system, ethanol was used to absorb the volatile organic matter. Notably, the reactions took place under an argon atmosphere. Afterwards, the generated black carbon material was refluxed in 200 mL, 20 wt %  $\text{HNO}_3$  for 4 h at 100 °C to remove impure and unstable species, this was followed by distilled water washing for several times, until the filtrate was close to neutral. At last, the residue from filtering was dried at 105 °C in an oven for 12 h, the obtained product was then labeled as Fe-CNT.

For the synthesis of Fe-N-CNTs, 0.2 g Fe-CNT and 1 g of melamine (i.e.  $\text{C}_3\text{N}_3(\text{NH}_2)_3$ ) were mixed uniformly and heated in quartz holder at 750 °C, 800 °C, 850 °C and 900 °C for 2h with Ar purging at a heating rate of 20 °C  $\text{min}^{-1}$ . Afterwards, cooling down to room temperature was performed naturally. The generated carbon powder was labeled as Fe-N-CNTX, where X represents the thermal annealing temperature.

The size and surface morphology of all catalysts were visualized with Field-Emission Transmission Electron Microscope (Tecnai G2 F20 S-TWIN) at an accelerating voltage of 200 kV. Transmission Electron Microscope (TEM), High Revolution Translation Electron Microscopy (HR-TEM), and High-Angle Annular Dark Field- Scanning Transmission Electron Microscope- Energy Dispersive Spectrometer (HAADF-STEM-EDS) images were taken on a JEM-2100F and Bruker super-X with an acceleration voltage of 200 kV. The specific surface areas, pore size distribution and pore volumes were determined using nitrogen adsorption-desorption measurements at 77 K, with the Brunauer-Emmett-Teller (BET), QSDFT methods and v-T method. The crystal structure was tested using X-ray diffraction (XRD) with a scanning step of 0.026° in the 2 $\theta$  range from 10° to 80° on a Philips X' Pert PRO. The carbon structure was recorded using Raman spectroscopy with an excitation wavelength of 532 nm from 200 to 3500  $\text{cm}^{-1}$  on LabRAM HR800. The surface chemical compositions were analyzed with X-ray photoelectron spectroscopy using Al K $\alpha$  line (15 kV, 10 mA, 150 W) as a radiation source on XPS, Axis Ultra DLD, Kratos.

The electrochemical measurements were conducted on an electrochemical workstation (CHI760E, CHINA) equipped with a three-electrode system, rotating disk electrode (RDE, ATA-1B, CHINA). The glassy carbon electrode (GCE) on RDE worked as the working electrode. The saturated calomel electrode (SEC) Hg/HgCl served as a reference electrode and a piece of Pt foil was used as the counter electrode.

Before the electrochemical test, each catalyst was mechanically grounded for 30 min to ensure that the powder particles were small enough to guarantee uniform distribution for the test. About 10 mg of catalyst was firstly dispersed in 40  $\mu\text{L}$  5 wt.% Nafion solution and then 100  $\mu\text{L}$  absolute ethanol was introduced into the solution. The mixed solution was stirred with an ultrasonic stirrer for 30 min to form a homogenous ink. For each test, 2  $\mu\text{L}$  of ink was deposited on the working electrode, and after air dried for 12 h, the ORR performance of the catalyst was tested in 0.1 M KOH aqueous solution. RDE cyclic voltammetry (CV) was performed in a  $\text{N}_2$ - and  $\text{O}_2$ -saturated solution with 10  $\text{mV s}^{-1}$  scan rate from -1 V to 0 V (vs SEC). RDE linear sweep voltammetry (LSV) was executed in a  $\text{O}_2$ -saturated solution with 5  $\text{mV s}^{-1}$  scan rate from -1 V to 0 V (vs SEC) at different rotation speeds ranging from 800 rpm to 2400 rpm. The stability of the catalysts was evaluated by the i-t in  $\text{O}_2$ -saturated solution for 40000 s. The methanol tolerance of the catalysts was performed in  $\text{O}_2$ -saturated solution with and without the presence of methanol.

The electrolyte solution was replaced after each electrochemical measurement, with a fresh one, to ensure reproducible results. All the potentials used in the tests were referred to the Hg/HgCl electrode and the potentials could be converted into reversible hydrogen electrode (RHE), according to the following equation:

$$E(\text{vs RHE}) = E(\text{vs SCE}) + 0.0591 \text{pH} + 0.24 \quad (1)$$

The electron transfer number  $n$  for all the catalysts was calculated by the Koutechy-Levich equation as reported below:

$$\frac{1}{J} = \frac{1}{J_L} + \frac{1}{J_K} = \frac{1}{B\omega^{1/2}} + \frac{1}{J_K} \quad (2)$$

$$B = 0.62nFC_0D_0^{2/3}\nu^{-1/6} \quad (3)$$

where  $J$ ,  $J_K$ , and  $J_L$  are respectively the measured current density, the kinetic current density and the diffusion-limited current density.  $\omega$  is the electrode rotation rate, and  $F$  is the Faraday constant ( $96485 \text{ C mol}^{-1}$ ),  $C_0$  is the bulk concentration of  $\text{O}_2$  ( $1.2 \times 10^{-3} \text{ mol L}^{-1}$  for 0.1 M KOH solution),  $D_0$  is the diffusion coefficient of  $\text{O}_2$  ( $1.9 \times 10^{-5} \text{ cm}^2 \text{ s}^{-1}$  for 0.1 M KOH solution), and  $\nu$  is the kinetic viscosity of the electrolyte ( $0.01 \text{ cm}^2 \text{ s}^{-1}$  for 0.1 M KOH aqueous solution).

For the Zn-air battery tests, the air electrode was prepared by coating the ink produced from the prepared electrocatalyst (Fe-N-CNT850) and the ink produced from the commercial one (20% Pt/C) onto hydrophobic carbon paper uniformly, whereas a piece of polished Zinc plate of the same size was used as anode and a solution of 6 M KOH containing 0.2 M zinc acetate was used as electrolyte. For each test, 16 mg catalyst, 2 mg acetyleneblack, and 2 mg pol (vinylidene fluoride) (PVDF) were mixed in N-methyl-2-pyrrolidone (NMP) to form a homogeneous slurry. The slurry was painted on carbon paper and dried at 60 °C for 6 h with a loading of  $0.1 \text{ mg cm}^{-2}$ , to be used as electrode.

## Results and Discussion

The characterization of the plastic waste is shown in **table S1**.

**Table S1.** Proximate analysis and ultimate analysis of polypropylene

Sample	Proximate analysis/% <sub>ar</sub>				Ultimate analysis (wt.-%) <sub>db</sub>			
	M	A	V	FC	C	H	S	O <sup>[a]</sup>
Polypropylene	0.037	0.056	99.871	0.036	85.180	13.737	0.169	0.858

[a] Calculated.

Figure S1 mainly shows the statistical distribution of iron particle size and outer diameter of carbon nanotubes and the corresponding standard deviations. The average outer diameters of carbon nanotubes and the iron nanoparticles in Fe-N-CNT850 are 16.0 nm and 10.8 nm, respectively. Furthermore, the large standard deviations of outer diameters mean broad distribution in diameter. On the contrary, much more uniform distribution of Fe particles size was obtained

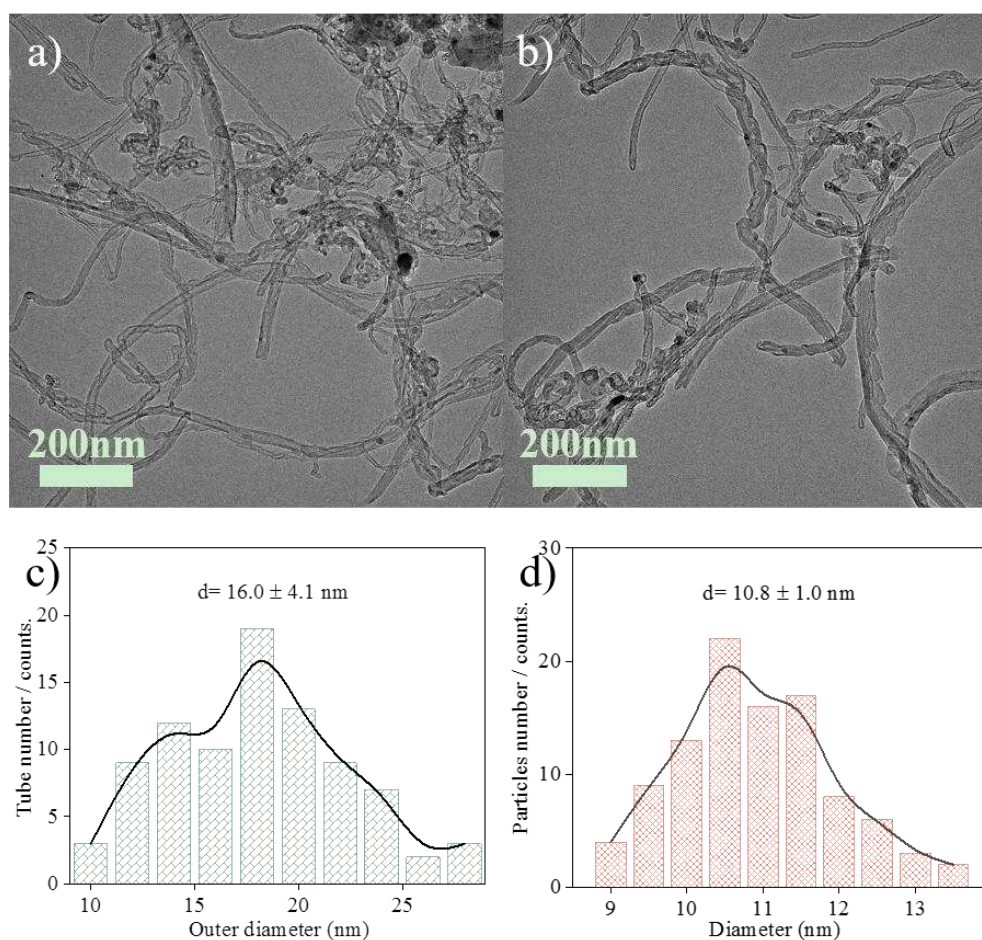
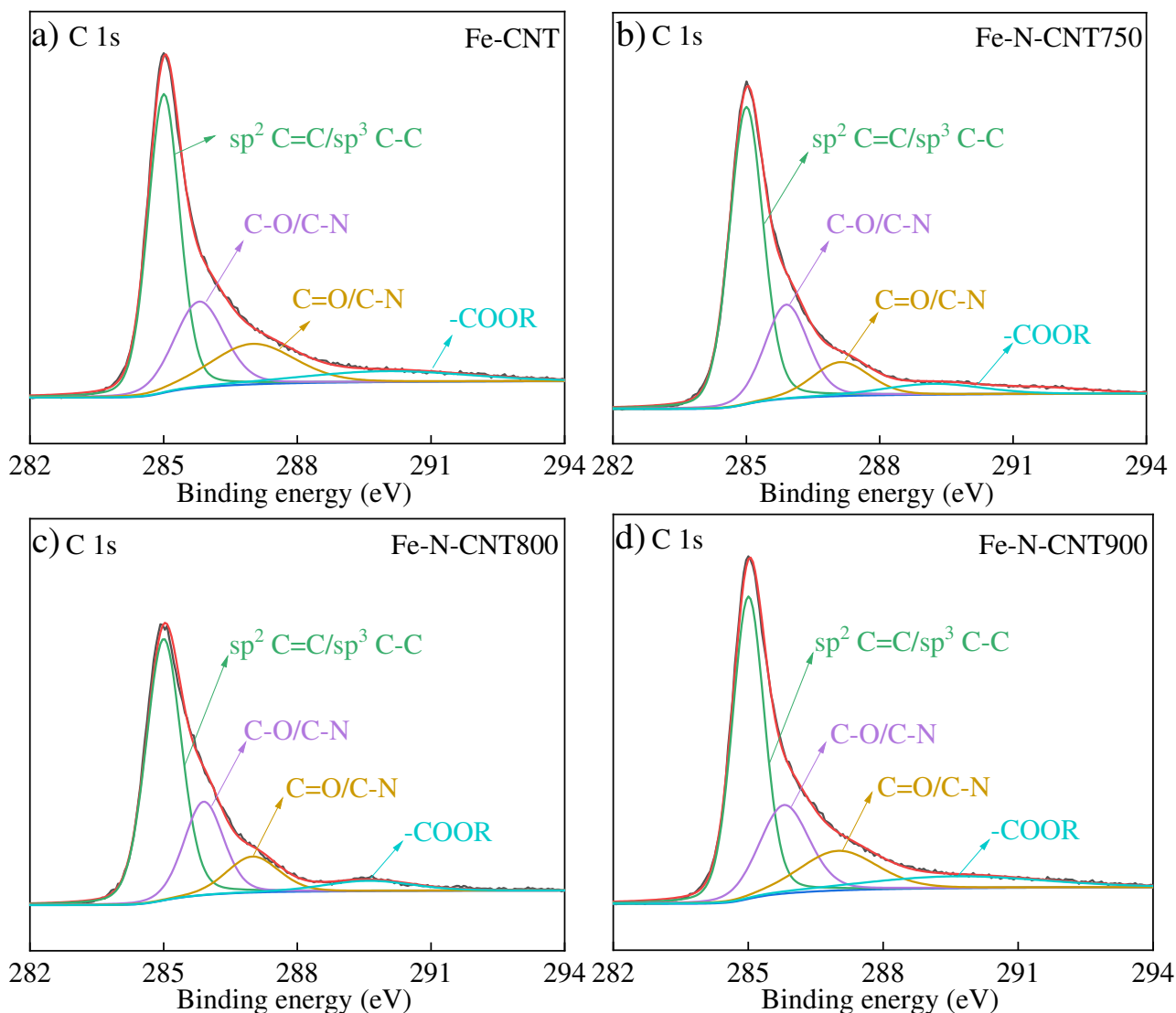


Figure S1 (a) TEM 1, (b) TEM 2, (c) distribution of the outer diameter and (d) diameter of Fe particles of Fe-N-CNT850.

Figure S2 shows the XPS spectra of other samples. Fe-CNT is obtained from the catalytic pyrolysis of polypropylene, using alumina loaded with iron. Fe-N-CNT750, Fe-N-CNT800 and Fe-N-CNT900 are obtained at different temperatures of co-pyrolysis of Fe-CNT with melamine.



**Figure S2.** C 1s XPS spectrum of Fe-CNT (a), Fe-N-CNT750 (b), Fe-N-CNT800 (c) and Fe-N-CNT900 (d).

Figure S3 shows the XPS spectra of other samples. Fe-CNT is obtained from the catalytic pyrolysis of polypropylene, using alumina loaded with iron. Fe-N-CNT750, Fe-N-CNT800 and Fe-N-CNT900 are obtained at different temperatures of co-pyrolysis of Fe-CNT with melamine.

While the C 1s XPS spectra appear to be quite similar, for the O 1s XPS spectra we see that the intensities of the oxygen bonds are deeply influenced by the temperature which changes the composition of the catalysts in terms of hydrogen, and oxygen. We can see as macroscopic effects:

- the reduction of chemisorbed oxygen and water with the increase of the temperature;
  - epoxy carbon (C-O-C) also tends to decrease with the increase of temperature;
  - while carbonyl carbon (C=O) and hydroxyl carbon (C-O) tend to increase at low temperatures, they decrease at high temperatures.
- This is due to a first dehydrogenation step which is followed by aromatic condensation which generally is responsible of the formation of aromatic compounds and the decrease of aliphatic compounds. This brings to a further graphitization of the nanotube, which importantly influences its electrical properties. Generally the O 1s peak of charcoal carbonized at higher temperatures gets small. The graphitization of the carbon nanotube brings to a decrease in the electrical resistivity of the material, due to the generation of  $\pi$ -electron system caused by aromatic condensation.

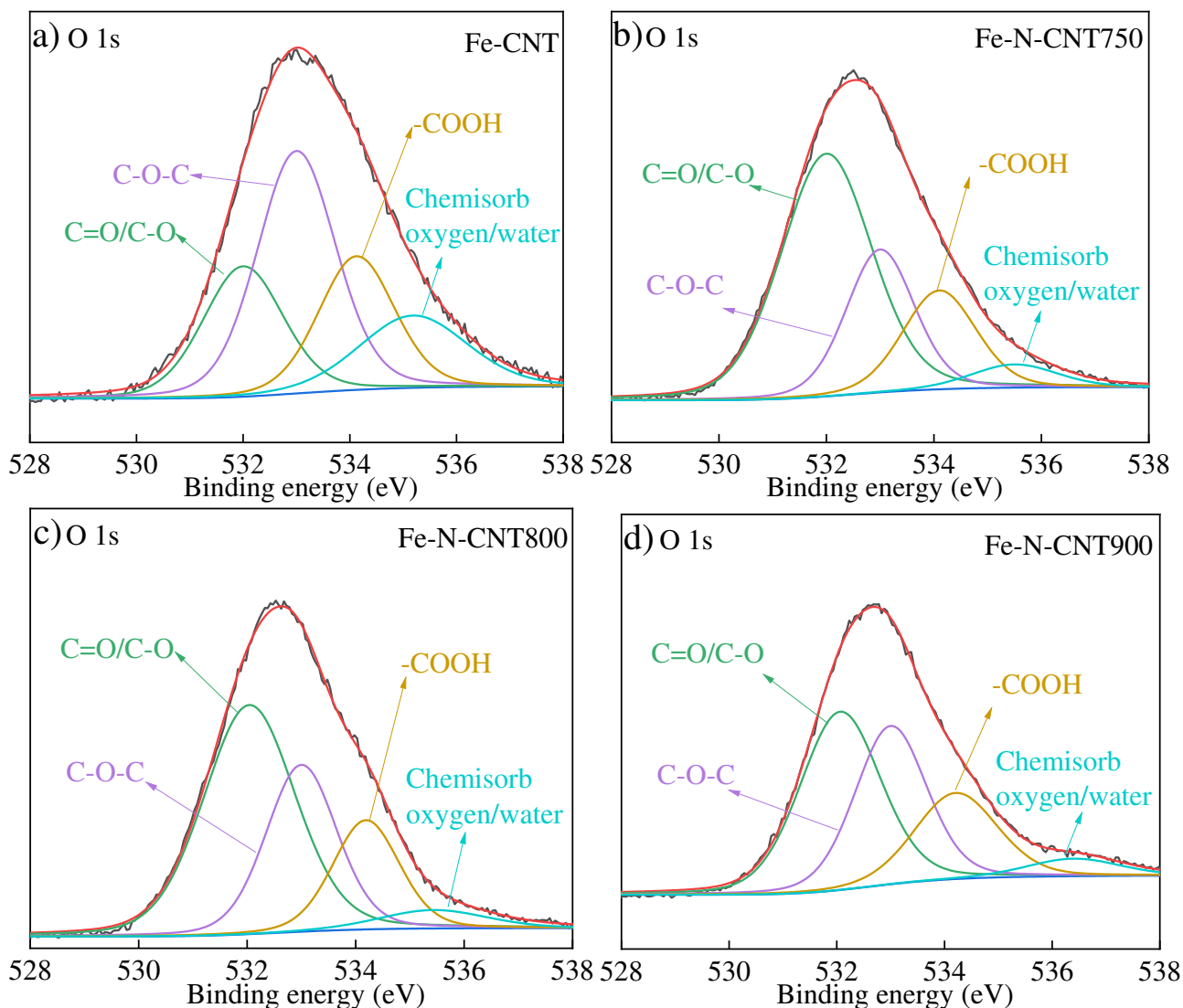


**Figure S3.** O 1s XPS spectrum of Fe-CNT (a), Fe-N-CNT750 (b), Fe-N-CNT800 (c) and Fe-N-CNT900 (d).

Based on the XPS diagrams and the fitted peaks the mass percentages of the carbon nitrogen and iron were calculated and are reported in the **table S2**. From this it can be seen that the initial carbon Fe-CNT has a higher content of carbon, while the co-pyrolysis with melamine seems to enrich the carbon nanotube with hydrogen and water. The presence of water is confirmed also by **figure S3**. The content of carbon of the Fe-N-CNTs increases with the increase of the co-pyrolysis temperature. The content of nitrogen and of iron also increase.

**Table S2.** Mass percentages of the elements obtained in the XPS survey spectra.

Sample	C wt.%	N wt.%	Fe wt.%
Fe-CNT	90.76	0.34	0.32
Fe-N-CNT750	79.26	0.70	1.17
Fe-N-CNT800	80.07	0.44	0.51
Fe-N-CNT850	84.02	0.69	0.84
Fe-N-CNT900	87.27	0.58	0.49

Figure S4 shows that the initial Fe-CNT catalyst has a porosity of about 500 cm<sup>3</sup>/g STP, while the electrocatalyst obtained at 750°C has a great increase in porosity reaching exactly 800 cm<sup>3</sup>/gSTP. The electrocatalysts obtained at temperatures equal to 800°C and 900°C have instead a reduced porosity, this is due to the fact that excessive temperature destructs the structure of the micropores, which collapse.

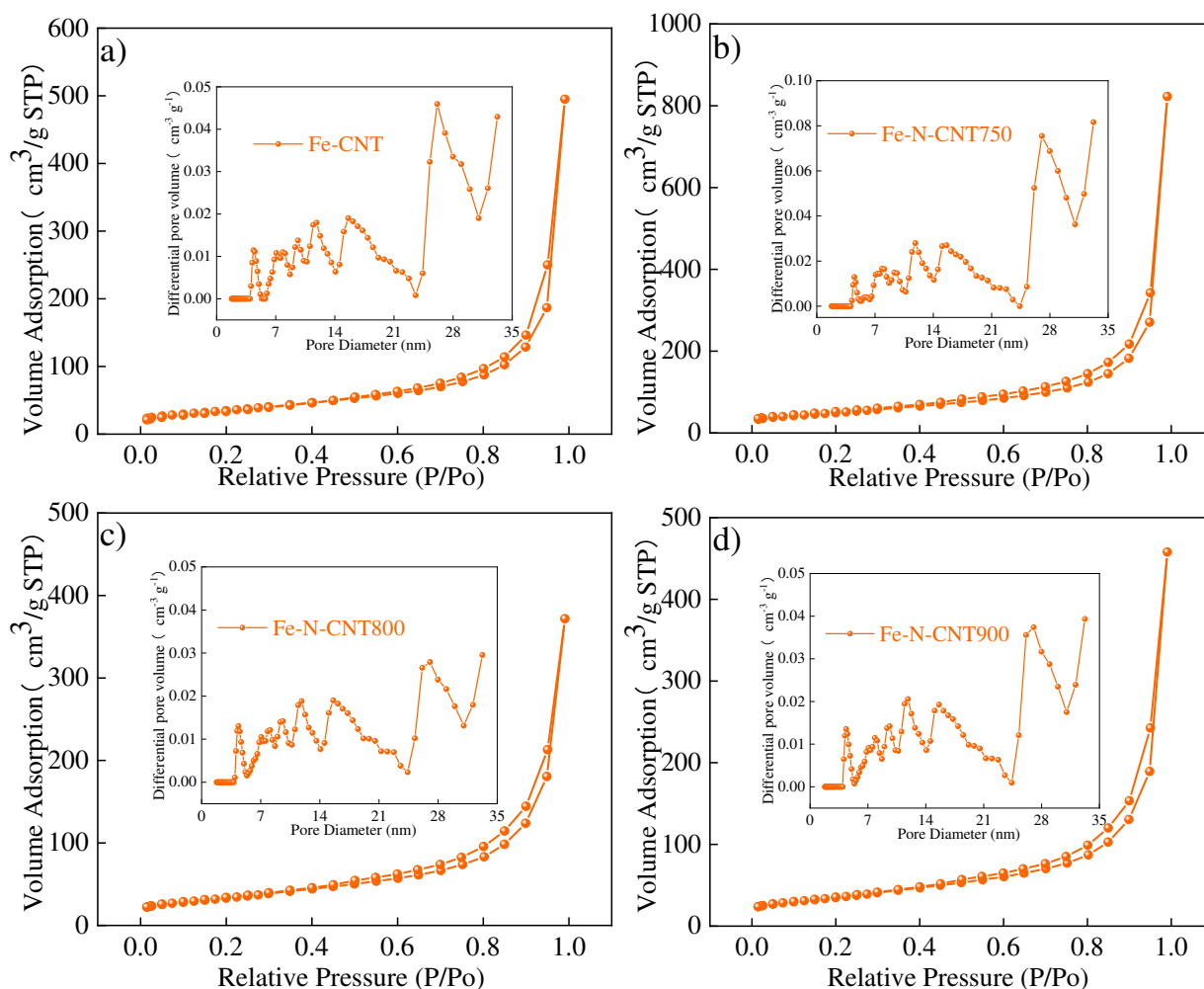


**Figure S4.** Nitrogen adsorption-desorption curves and pore size distribution of Fe-CNT (a), Fe-N-CNT750 (b), Fe-N-CNT800 (c) and Fe-N-CNT900 (d)..

A summary of the textural parameters obtained from the  $S_{\text{BET}}$  analysis are reported in table S3.

**Table S3.** Textural parameters of the materials.

Sample	$S_{\text{BET}}$ (m <sup>2</sup> /g)	$D_{\text{ave}}$ (nm)	$V_t$ (cm <sup>3</sup> /g)
Fe-CNT	126.1	24.3	0.77
Fe-N-CNT750	178.7	28.5	1.28
Fe-N-CNT800	120.3	19.2	0.58
Fe-N-CNT850	114.4	24.7	0.71
Fe-N-CNT900	127.4	22.3	0.71

The data shown in the table S3 confirm those shown in figure S4. We see a reduction in the surface area passing from a temperature of 750°C to a temperature of 900°C. This corresponds also to a reduction of the average diameter of pores and also to a reduction in the total volume of the pores ( $V_t$ ).

In figure S5 the CV curves of all the electrocatalysts are shown. Their behaviour is compared with that of 20% Pt/C. It can be seen that the electrocatalyst Fe-N-CN850 is the one which has more similar performance respect to 20%Pt/C. All the electrocatalysts result to have a peak about 0.8 V which corresponds to the reduction reaction, as reported for other tests performed with similar carbonaceous material [1].

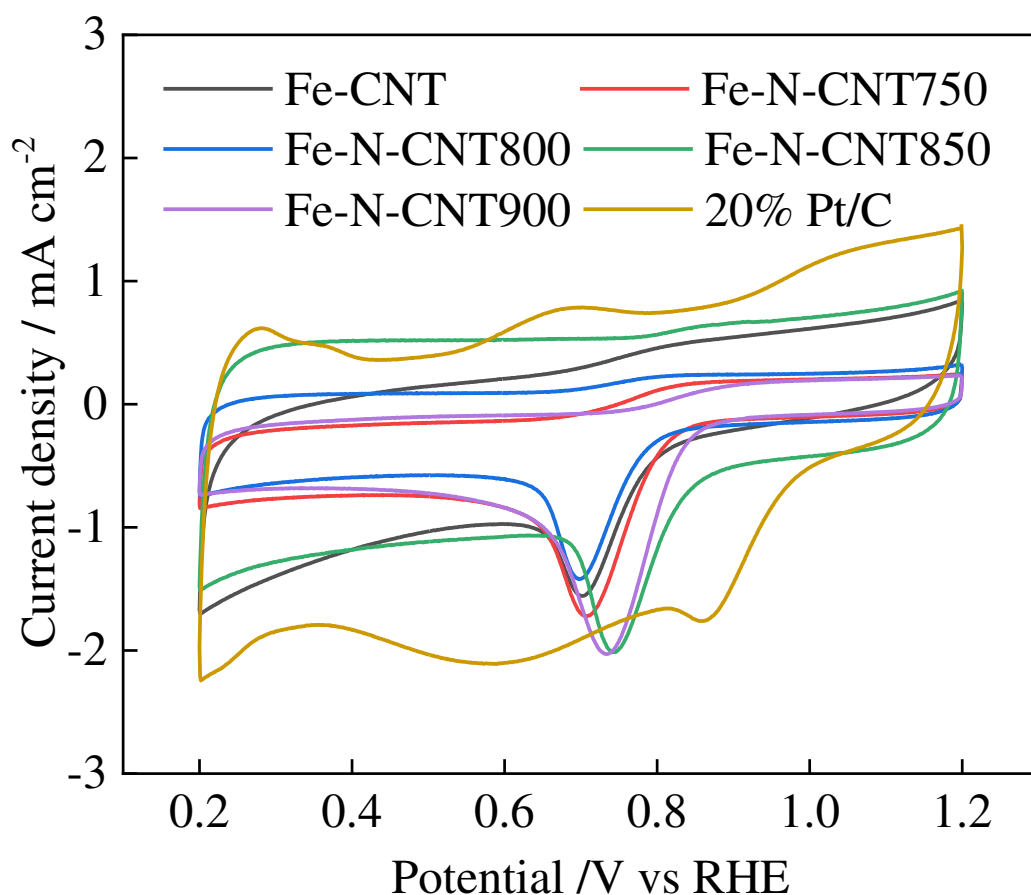


Figure S5. CV curves of all electrocatalysts.

In table S4 the onset potential and halfwave potential of the electrocatalysts are reported. Compared with commercial platinum on carbon (Pt/C), the optimized catalyst obtained from pyrolysis at 850°C, showed remarkable electrocatalytic properties with onset potential of 0.943 V vs RHE and half-wave potential of 0.811 V vs RHE and even better stability and anti-poisoning.

Table S4. Onset potential and halfwave potential.

Sample	Fe-CNT	Fe-N-CNT750	Fe-N-CNT800	Fe-N-CNT850	Fe-N-CNT900	20% Pt/C
Onset potential (V)	0.806	0.877	0.874	0.943	0.898	0.969
Halfwave potential (V)	0.655	0.715	0.747	0.811	0.772	0.850

Figure S6 shows the different rotation rates LSVs and K-L plots, and transfer electron numbers of other catalysts. And the transfer electron numbers were much lower than that of Fe-N-CNT850.

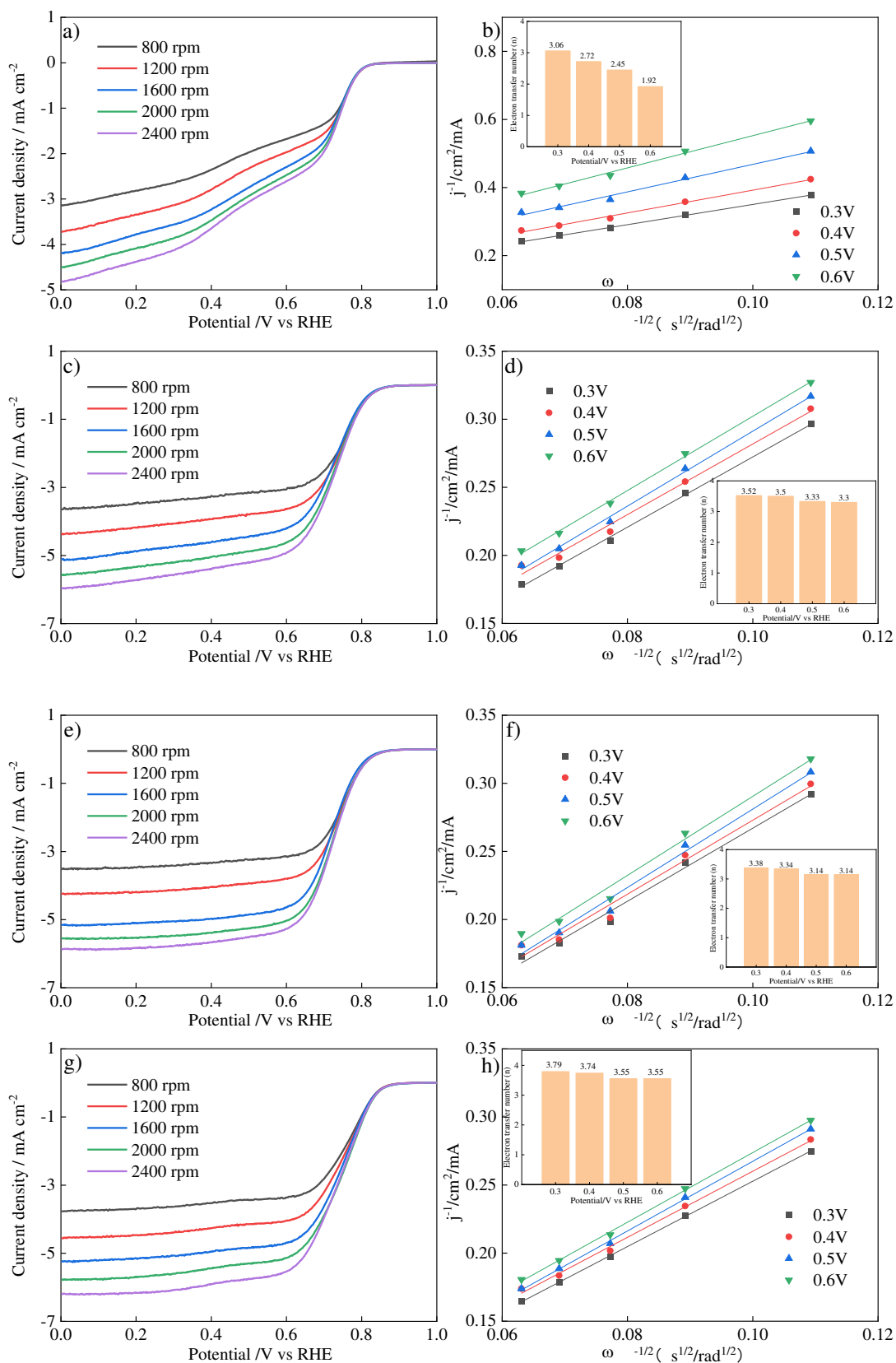


**Figure S6.** Different rotation rate LSVs, K-L plots and transfer electron of Fe-CNT (a, b), Fe-N-CNT750 (c, d), Fe-N-CNT800 (e, f) and Fe-N-CNT900 (g, h).

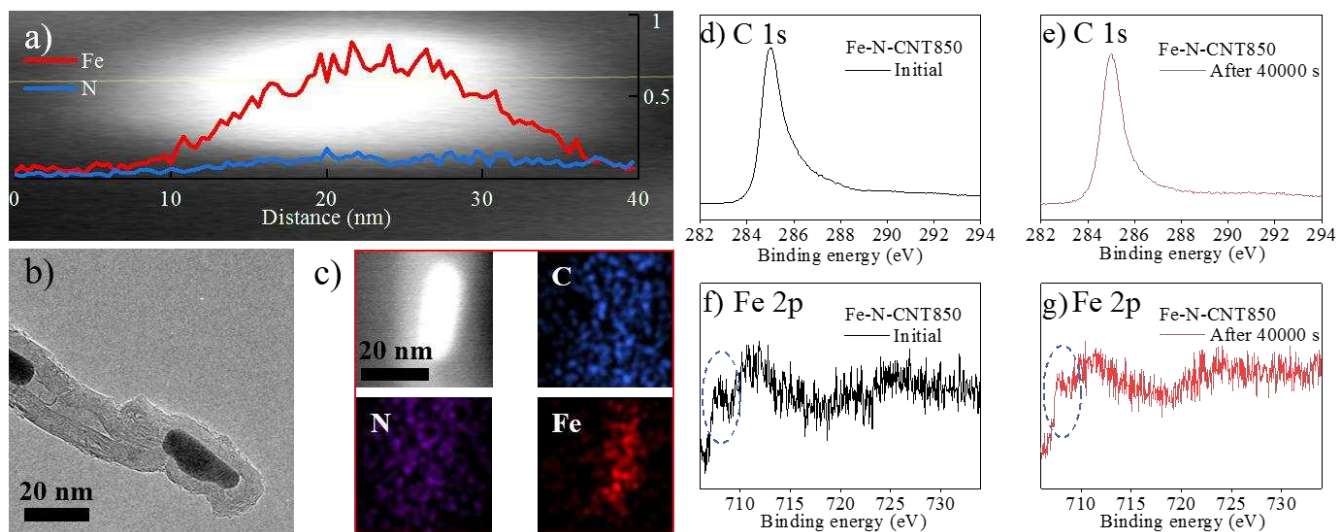


Figure S7. (a) HAADF-STEM cross-sectional compositional profiles. (b) HR-TEM image showing the presence of metal nanoparticles inside of carbon layers. (c) HAADF-STEM images with elemental mapping of C, N and Fe. (d) high-resolution XPS spectrum of C 1s for initial Fe-N-CNT850. (e) high-resolution XPS spectrum of C 1s for Fe-N-CNT850 after stability test. (f) high-resolution XPS spectrum of Fe 2p for initial Fe-N-CNT850. (g) high-resolution XPS spectrum of Fe 2p for Fe-N-CNT850 after stability test.

**Table S5.** Comparison of electrochemical activity of Fe-N-CNTs to the other reported ORR catalysts in alkaline electrolyte.

Catalysts	Onset potential (V vs. RHE)	halfwave potential (V vs. RHE)	Reference
Fe-N-CNT850	0.943	0.811	This work
AA-Fe <sub>2</sub> N@NC	0.927	0.828	S[1]
CNT@f-FeNC170	0.97	0.84	S[2]
Fe-N-C	-	0.80	S[3]
Fe-N-C/rGO	0.94	0.81	S[4]
(FeCo@N-GCNT-FD)	0.96	0.88	S[5]
Fe/N-S-CNTs	-	0.836	S[6]
Fe-N-C	-	0.818	S[7]
aFe-NGC-650	0.99	0.85	S[8]
Fe-UFC/MnO <sub>2</sub>	0.95	0.79	S[9]
Fe-N-C@CNT	0.915	0.827	S[10]
Fe <sub>3</sub> N@N-C	0.995	0.849	S[11]
N-CNT-900	0.94	0.80	S[12]
Fe-N/N-C pNFs	0.95	0.78	S[13]
3D Fe/N-G#6	0.976	0.828	S[14]

## References

- [1] A. Zhu, L. Qiao, P. Tan, Y. Ma, W. Zeng, R. Dong, C. Ma, J. Pan, *Appl. Catal. B: Environ.*, 254 (2019), pp. 601-611
- [2] G. Zhang, Y. Jia, C. Zhang, X. Xiong, K. Sun, R. Chen, W. Chen, Y. Kuang, L. Zheng, H. Tang, W. Liu, J. Liu, X. Sun, W. Lin, H. Dai, *Energy Environ. Sci.*, 12 (2019), pp. 1317-1325
- [3] Z. Zhang, J. Sun, F. Wang, L. Dai, *Angew. Chem., Int. Ed.*, 57 (2018), pp. 9038-9043
- [4] Zhang, C., Liu, J., Ye, Y., Aslam, Z., Brydson, R., Liang, C., , *ACS Appl. Mater. Interfaces*, 10 (2018), pp. 2423-2429
- [5] L. An, N. Jiang, B. Li, S. Hua, Y. Fu, J. Liu, W. Hao, D. Xia, Z. Sun, *J. Mater. Chem. A*, 6 (2018), pp. 5962-5970
- [6] C. Lai, J. Wang, W. Lei, C. Xuan, W. Xiao, T. Zhao, T. Huang, L. Chen, Y. Zhu, D. Wang, *ACS Appl. Mater. Interfaces*, 10 (2018), pp. 38093-38100
- [7] L. Wang, L. Fu, J. Li, X. Zeng, H. Xie, X. Huang, H. Wang, Y. Tang, , *J. Mater. Sci.*, 53 (2018), pp. 10280-10291
- [8] X. Li, Y. Zhang, J. Zhang, C. Wang, *Nanoscale*, 11 (2019), pp. 23110-23115
- [9] Y. Wang, F. Wang, Y. Fang, J. Zhu, H. Luo, J. Qi, W. Wu, *Appl. Surf. Sci.*, 496 (2019), pp. 143566
- [10] J. Zhang, Y. Zhao, K. Hou, C. Wu, L. Guan., *Nanotechnol.*, 30 (2019), pp. 485705
- [11] T. Li, M. Li, M. Zhang, X. Li, K. Liu, M. Zhang, X. Liu, D. Sun, L. Xu, Y. Zhang, Y. Tang., *Carbon*, 153 (2019), pp. 364-371
- [12] D. Liu, Li, J. C., Shi, Q., Feng, S., Lyu, Z., Ding, S., Hao, L., Zhang, Q., Wang, C., Xu, M., Li, T., Sarnello, E., Du, D., Lin, Y., *ACS Appl. Mater. Interfaces*, 11 (2019), pp. 39820-39826
- [13] M. Sun, Z. Xie, Z. Li, X. Deng, Q. Huang, Z. Li, *Int. J. Hydrogen Energy*, 44 (2019), pp. 24617-24627
- [14] C. Wang, Z. Li, L. Wang, X. Niu, S. Wang., *ACS Sustainable Chem. Eng.*, 7 (2019), pp. 13873-13885

## Author Contributions

Professor Hanping Chen, professor P.T. Williams and professor Haiping Yang developed the innovative technology for carbon nanotubes preparation and secured the fundings. Cai Ning, Sunwen Xia and Xiong Zhang contributed to the preparation of the catalysts through pyrolysis experiments; Zihan Meng contributed to the characterization of the electrocatalysts. Yingquan Chen, dr. Pietro Bartocci and prof. Francesco Fantozzi supervised and controlled the results.